Molecular Cell, Vol. 11, 577–590, March, 2003, Copyright ©2003 by Cell Press

p53 Has a Direct Apoptogenic Role at the Mitochondria

Motohiro Mihara,[1,4] Susan Erster,[1,4] Alexander Zaika,[1] Oleksi Petrenko,[1] Thomas Chittenden,[2] Petr Pancoska,[3] and Ute M. Moll[1,*]

[1]Department of Pathology
Stony Brook University
Stony Brook, New York 11794
[2]ImmunoGen, Inc.
128 Sidney Street
Cambridge, Massachusetts 02139
[3]Department of Chemistry
University of Illinois at Chicago
Chicago, Illinois 60607

Summary

p53 induces apoptosis by target gene regulation and transcription-independent signaling. However, a mechanism for the latter was unknown. We recently reported that a fraction of induced p53 translocates to the mitochondria of apoptosing tumor cells. Targeting p53 to mitochondria is sufficient to launch apoptosis. Here, we provide evidence that p53 translocation to the mitochondria occurs in vivo in irradiated thymocytes. Further, we show that the p53 protein can directly induce permeabilization of the outer mitochondrial membrane by forming complexes with the protective BclXL and Bcl2 proteins, resulting in cytochrome c release. p53 binds to BclXL via its DNA binding domain. We probe the significance of mitochondrial p53 and show that tumor-derived transactivation-deficient mutants of p53 concomitantly lose the ability to interact with BclXL and promote cytochrome c release. This opens the possibility that mutations might represent "double-hits" by abrogating the transcriptional and mitochondrial apoptotic activity of p53.

Introduction

The basis for p53's striking apoptotic and tumor suppressive potency lies in its pleiotropism, which includes transcription-dependent and -independent functions. p53 kills cells predominantly via the mitochondrial death pathway (reviewed in Johnstone et al., 2002). p53 can mediate apoptosis by transcriptional activation of pro-apoptotic genes like the BH3-only proteins Noxa and Puma, Bax, p53 AIP1, Apaf-1, and PERP and by transcriptional repression of Bcl2 and IAPs (references in Johnstone et al., 2002). For Noxa, Puma, and PIDD, downregulation decreases—but does not abolish—the extent of death after stress. Of note, induction of these target gene products shows variable kinetics, with some being delayed in their response (over 24 hr), e.g., Bax and p53AIP1 (Nakano and Vousden, 2001; Attardi et al., 2000). Analysis of p53-regulated global gene expression shows that the type, strength, and kinetics of the target gene profiles depend on p53 levels, stress type, and cell type (Zhao et al., 2000). This indicates that only individual genes will be chosen from the complex spectrum of potentially inducible genes to mediate a specific p53 response in a given physiological situation.

In addition, evidence for transcription-independent p53-mediated apoptosis has been accumulating. In some cell types, p53-dependent apoptosis occurs in the absence of any gene transcription or translation (Caelles et al., 1994; Wagner et al., 1994; Gao and Tsuchida, 1999). Also, inhibitors of protein phosphatases induce p53-dependent death in the absence of transactivation (Yan et al., 1997). Moreover, the transcriptionally inactive p53 mutants (1–214) and p53 22/23QS act as potent death inducers in tumor cells (Haupt et al., 1995; Chen et al., 1996; Kokontis et al., 2001). In (mitochondria-containing) cell-free S100 extracts that model p53-dependent but transcription-independent apoptosis, p53 protein directly mediates caspase-3 activation, and immunodepletion of p53 completely blocks this activity. This pathway requires caspase 8 activation (Ding et al., 2000). Also, in cell-free cytoplasts, activation of cytosolic p53 can induce mitochondrial cytochrome c release (Schuler and Green, 2001). Together, these data indicate the coexistence of a transcription-independent pathway of p53-mediated apoptosis. However, the underlying mechanism of action remained unknown.

Mitochondria are central death regulators in response to DNA damage, growth factor withdrawal, hypoxia, and oncogene deregulation and are critical for p53-dependent death (Wang, 2001). When mitochondria receive a death signal, the outer mitochondrial membrane (OMM) undergoes permeabilization, which causes the release of potent death factors from the intermembraneous space into the cytosol (Green and Evan, 2002). These apoptogenic factors activate caspase-9 (cytochrome c), inhibit cytosolic IAPs (Smac, Htra2), induce chromatin condensation (AIF), or degrade DNA (Endonuclease G). OMM permeabilization is regulated by the opposing actions of pro- and antiapoptotic Bcl2 proteins, although the exact mechanism of how the Bcl2 family controls OMM permeability is unclear. The antiapoptotic members, typified by Bcl2 and BclXL, constitutively reside at the OMM and mediate a critical pro-survival function by stabilizing the OMM and preventing the release of death factors. Overexpressed Bcl2 and BclXL suppress p53-dependent and -independent cell death. The pro-apoptotic members consist of the BH3-only class, which regulates the protective Bcl2/XL proteins, and the multi-domain BH123 class. The type II BH3-only proteins Noxa, Puma, Bik, Bim, and Bad couple death signals to mitochondria and in healthy cells are sequestered to cytosolic sites other than the OMM. Upon sensing death stimuli, BH3-only proteins undergo posttranslational modifications and mitochondrial translocation (reviewed in Huang and Strasser, 2000). Translocated BH3-only proteins then bind to Bcl2/XL via their BH3 domain, thereby inactivating their protective function (Cheng et al., 2001). In resting cells, BH123 proteins exist as inac-

*Correspondence: umoll@notes.cc.sunysb.edu
[4]These authors contributed equally to this work.

tive monomers in the cytosol (Bax) or at mitochondria (Bak) (Wolter et al., 1997) and can be induced to homo-oligomerize and insert into the OMM by tBid after death stimuli, leading to cytochrome c release (Wei et al., 2000; Eskes et al., 2000). BH3-only proteins are upstream of BH123 proteins since Bax/Bak double null cells are resistant to Bim- and Bad-induced apoptosis (Zong et al., 2001).

In search of the basis for transcription-independent p53-mediated death, we recently found that a fraction of induced wild-type p53 (wt) rapidly translocates to the mitochondrial surface of cultured tumor cells. Bypassing the nucleus by targeting p53 to mitochondria is sufficient to induce marked death in p53-deficient tumor cells, indicating that p53 can launch apoptosis directly from mitochondria (Marchenko et al., 2000). Here, we show that wtp53 protein directly induces mitochondrial permeabilization and cytochrome c release by forming inhibitory complexes with the protective BclXL and Bcl2 proteins. p53 binds to BclXL via its DNA binding domain. Tumor-derived p53 mutants are incapable or severely impaired in forming BclXL complexes and releasing cytochrome c. These data argue for an in vivo role of mitochondrial p53 and suggest that missense mutations in tumors might select against *both* the transcriptional and the mitochondrial apoptotic activity of p53.

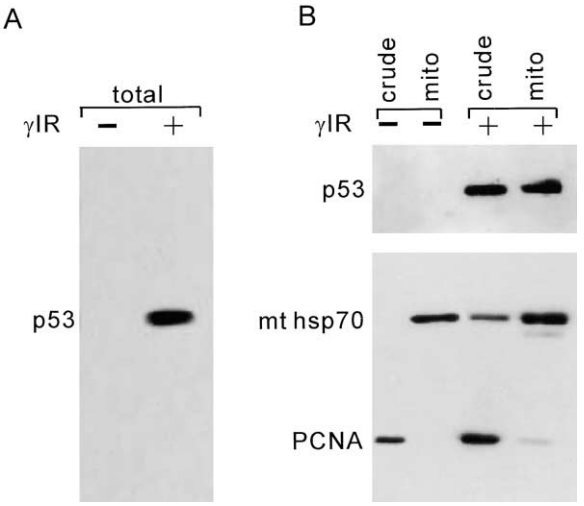

Figure 1. p53 Rapidly Accumulates at Mitochondria during γIR-Induced Apoptosis in Primary Thymocytes

Mouse thymocytes were either mock treated (−) or irradiated with 10 Gy (+).

(A) p53 immunoblot from whole-cell lysates.

(B) p53 immunoblot of crude cell or mitochondrial lysates. Membrane was reblotted with α-PCNA as nuclear contamination marker and α-mt hsp70 as mitochondrial marker (5 μg total protein per lane in all).

Results

p53 Rapidly Accumulates at Mitochondria of Primary Thymocytes Undergoing γIR-Induced Apoptosis

We recently reported that a fraction of stress-induced wild-type p53 translocates to mitochondria during p53-dependent apoptosis after DNA damage and hypoxia. This phenomenon occurs in all malignant and immortal human and mouse cell lines tested. We estimate that the amount of induced mitochondrial p53 in camptothecin-treated ML-1 cells is about equimolar to induced nuclear p53, based on total mitochondrial to nuclear protein and volume ratios. In contrast, wtp53 does *not* translocate during p53-*in*dependent apoptosis or p53-mediated cell cycle arrest. Mitochondrial p53 translocation occurs early (within 1 hr after a death stimulus) and precedes changes in mitochondrial membrane potential, cytochrome c release, and procaspase-3 activation (Marchenko et al., 2000). Suborganellar localization shows that p53 is predominantly located at the mitochondrial surface. This association can be reproduced in vitro with recombinant p53 and isolated mitochondria from unstressed cells (Sansome et al., 2001). To determine whether death-stimulus-induced mitochondrial p53 translocation also occurs in primary cells, we analyzed mouse thymocytes, which are the classic model for DNA damage-induced, p53-dependent cell death. γIR induces marked apoptosis in over 80% of thymocytes within 24 hr (Lowe et al.,1993). Freshly harvested thymocytes from young C57BL/6 mice were irradiated with 10 Gy or mock treated. Total cellular p53 became readily detectable after 1 hr, compared to undetectable levels prior to treatment (Figure 1A). Concomitant with total p53 induction, a fraction of p53 reproducibly translocated to mitochondria within 1 hr (Figure 1B), supporting an in vivo role of the p53 mitochondrial pathway.

Mitochondrially Targeted p53 Lacks Transactivation Activity and Suppresses Colony Formation

Bypassing the nucleus by targeting p53 to mitochondria is *sufficient* to induce marked apoptosis of p53-deficient tumor cells (SaOs2, HeLa, and H358) in the absence of additional DNA damage. This establishes the proof-of-principle that p53 can launch apoptosis directly from the mitochondrial platform (Marchenko et al., 2000, and our unpublished data). Nuclear bypassing was achieved by fusing the prototypical mitochondrial import leader of ornithin transcarbamylase to the N terminus of wtp53 (Lp53wt). Ectopic proteins with this leader are recognized at the mitochondrial surface, transported across the double membranes followed by enzymatic removal of the leader in the matrix, and resorted into their final submitochondrial compartments (membranes, intermembranous space, or matrix). Mitochondrial targeting of Lp53wt was verified by colocalization with mitochondrial markers in confocal microscopy and by cleavage of the leader peptide by endogenous mitochondrial endopeptidase (Marchenko et al., 2000). Lp53wt was undetectable in nuclei of transfected cells (Figure 2A), suggesting lack of transcriptional activity. To definitively rule out transcriptional activity of Lp53wt, we performed sensitive p53 reporter assays with PG13-Luciferase in p53 null H1299 and HeLa cells. In both lines, Lp53wt reproducibly showed lack of transactivation activity (Figure 2B, top), at equal expression with nuclear wtp53 (Figure 2B). To further exclude transcription function of Lp53wt, we compared the abilities of Lp53wt to nuclear wtp53 in inducing endogenous target genes of the apoptotic and arrest categories. Indeed, Lp53wt is unable to induce endogenous Noxa, Bax, and p21Waf1 proteins in H1299 cells (Figure 2B, bottom). Although the level

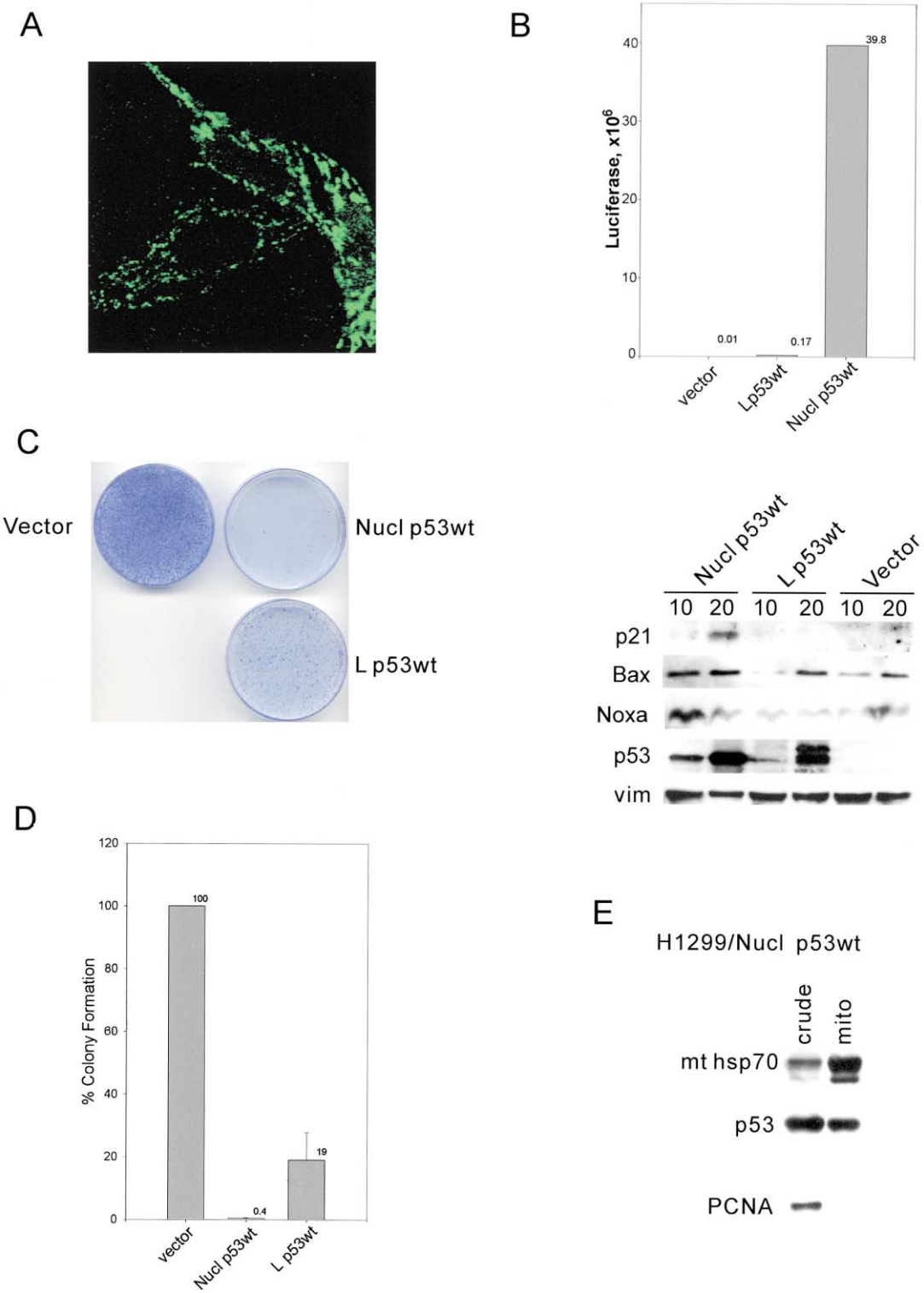

Figure 2. Mitochondrially Targeted p53 Lacks Transactivation Activity and Suppresses Colony Formation

(A) HeLa cells transfected with Flag-tagged Lp53wt and stained with Flag antibody (epifluorescence). Exclusive mitochondrial localization with nuclear sparing is apparent.

(B) Mitochondrially targeted Lp53wt lacks transactivation activity. (Top) p53 reporter assay in H1299 cells using the PG13 Luc reporter and 500 ng of each plasmid. (Bottom) Lp53wt fails to transactivate endogenous p53 targets such as p21, Bax, and Noxa. Western blots comparing induction by nuclear wtp53, Lp53wt, and empty vector in H1299 cells 10 and 20 hr after transfection (25 μg protein per lane). The Bax membrane was reblotted for vimentin (loading control) and for p53 expression. The upper band of Lp53wt is the fusion protein.

(C) Colony suppression assay of SaOs2 cells transfected with the indicated plasmids. After G418 selection for 18 days, cells were fixed and stained.

(D) Colony suppression assays from three independent experiments +/− SD.

(E) Mitochondrial translocation of nuclear wtp53 in transiently transfected H1299 cells. Whole-cell or mitochondrial lysates were blotted with α-p53, α-PCNA, and α-mthsp70 antibodies (10 μg per lane).

of Bax protein increased after 20 hr with Lp53wt, this is a nonspecific effect of transfection, since the same increase occurred with vector alone. Together, these data confirm the specificity of targeting and demonstrate that the apoptotic potency of targeted p53 is not due to a cryptic transcription-dependent p53 function but rather to a transcription-independent function at the mitochondria.

We next asked whether mitochondrially targeted p53 is also capable of exerting long-term growth suppression. In clonogenic survival assays of p53-deficient SaOs2 cells, targeted p53, although not as strong as nuclear p53, shows significant suppression compared to vector (set as 100%) (Figures 2C and 2D). To determine whether nuclear p53 also engages the mitochondrial pathway for colony suppression, in addition to the transcriptional pathway, we isolated mitochondria from cells transfected with nuclear wtp53. As seen in Figure 2E, mitochondrial translocation of transfected nuclear p53 is readily detected in HeLa and H1299 cells. This further supports the notion that the mitochondrial pathway participates in p53-mediated apoptosis and might explain the higher suppression efficiency of nuclear wtp53 with its "double" efficacy, engaging both nuclear and mitochondrial death pathways.

A Functional Link between p53 and Antiapoptotic Bcl Members

Several lines of evidence argue for a protein-protein interaction at the OMM as the underlying proapoptotic mechanism of mitochondrial p53: (1) Stimulus-induced endogenous p53 mainly translocates to the surface of mitochondria; (2) This surface association can be reproduced in vitro with recombinant p53 and unstimulated mitochondria (Sansome et al., 2001); (3) Truncation of the entire p53 C terminus is dispensable for its mitochondrial apoptotic action, arguing for a protein-protein interaction (Marchenko et al., 2000). In contrast, when p53 acts as a transcription factor, it depends on the ability to form tetramers via its C terminus (Friedman et al., 1993). Based on the surface location of mitochondrial p53, we looked for a link to the Bcl family of death regulators. The protective Bcl2 and BclXL proteins are particularly attractive candidates for p53 interaction since they are constitutively anchored at the OMM and mediate a critical survival function by stabilizing mitochondrial membranes and inhibiting release of cytochrome c and other apoptogenic factors (Green and Evan, 2002).

p53 Forms a Specific Complex with BclXL and Bcl2

To look for such complexes, we cotransfected Lp53wt with BclXL into p53 null H1299 cells for coimmunoprecipitations. Indeed, specific p53/BclXL complexes were readily detectable from transfected lysates by immunoprecipitating with anti-p53 antibodies DO-1 or 1801 and blotting with anti-BclXL (Figure 3A, lanes 2 and 3). No complexes were seen with irrelevant antibodies against abundant nuclear or mitochondrial proteins such as PCNA and mt hsp60 (lanes 4 and 5). The same complex was also seen in reverse (lane 7) and in cotransfected HeLa cells coexpressing BclXL and either targeted (Figure 3B, lane 1) or nuclear wtp53 (lane 3). In contrast, the identically targeted control transcription factor cRel (LcRel) failed to form a complex (lane 4). Moreover, this control shows that the p53/BclXL complex is not an artifact of the targeting motif, forced overexpression, or colocalization of proteins at the mitochondria. Of note, no complex was detectable between targeted p53 and Bax (lanes 6 and 8). In fact, even after triple transfection of targeted p53, BclXL, and Bax, no p53/Bax complex was seen (lane 10), while the p53/BclXL complex readily formed in the presence of Bax (lane 12), ruling out a triple complex. Also, Bax is unable to interfere with the formation of targeted or nuclear p53/BclXL complexes. In cotransfections, the amount of p53/BclXL complexes was the same in the absence or presence of exogenous Bax (Figure 3C). Given the structural similarity between BclXL and Bax proteins, this is the most stringent specificity control for the p53/BclXL complex. Since BclXL and Bcl2 share high structural and functional homology, a p53/Bcl2 complex might also be expected. Indeed, when HeLa cells were cotransfected with Lp53wt and Bcl2, a specific p53/Bcl2 complex was observed (Figure 3D, lane 3). No p53 complex was seen with Bax or PCNA (lanes 1 and 2), despite the fact that HeLa cells express readily detectable endogenous levels of both proteins. To demonstrate direct binding between p53 and BclXL, we did in vitro pull-down assays. A specific complex was pulled down with glutathione sepharose beads when purified baculoviral p53 was mixed with recombinant GST-BclXL but not with GST alone (Figure 3E, left). Also, inversely, when histidine-tagged p53 was incubated with GST-BclXL plus excess free GST, only GST-BclXL was captured by a Nickel column (Figure 3E, right).

To test whether such complexes also exist in vivo between endogenous proteins, we did coimmunprecipitation assays on solubilized mitochondria from wtp53-harboring ML-1 and RKO cells after short-term DNA damage by camptothecin. Mitochondrial isolates were free of nuclear contamination as verified by the PCNA marker (Figure 4C). Specific endogenous complexes of p53/BclXL and p53/Bcl2 were detected when extracts were precipitated with anti-BclXL (Figure 4A, lanes 1, 7, and 8) or anti-Bcl2 (Figure 4B, lane 5) and blotted with anti-p53 or, inversely, when extracts were precipitated with anti-p53 and blotted with anti-BclXL (Figure 4A, lane 3) or anti-Bcl2 (Figure 4B, lane 1). Moreover, when solubilized mitochondria were separated into supernatant and membrane-containing pellet, endogenous p53/BclXL complexes were present in both fractions, but were more abundant in the pellet extract (Figure 4A, compare lanes 7 and 8, note different input). Again, no endogenous p53/Bax complex was found (Figure 4A, lane 10), confirming specificity of the endogenous complexes. The absence of a p53/Bax complex also suggests that mitochondrial p53 and Bax promote apoptosis in a functionally synergistic but distinct manner; hence cooperativity might be expected. Consistent with this notion, we found synergism between targeted p53 and Bax in apoptosis, since cotransfected cells showed increased and earlier apoptosis (Figure 4D).

p53 Targeted to Mitochondria via the Bcl2 Transmembrane Domain Also Promotes Apoptosis

To further prove the functional significance of the p53-BclXL interactions, we exploited the transmembrane do-

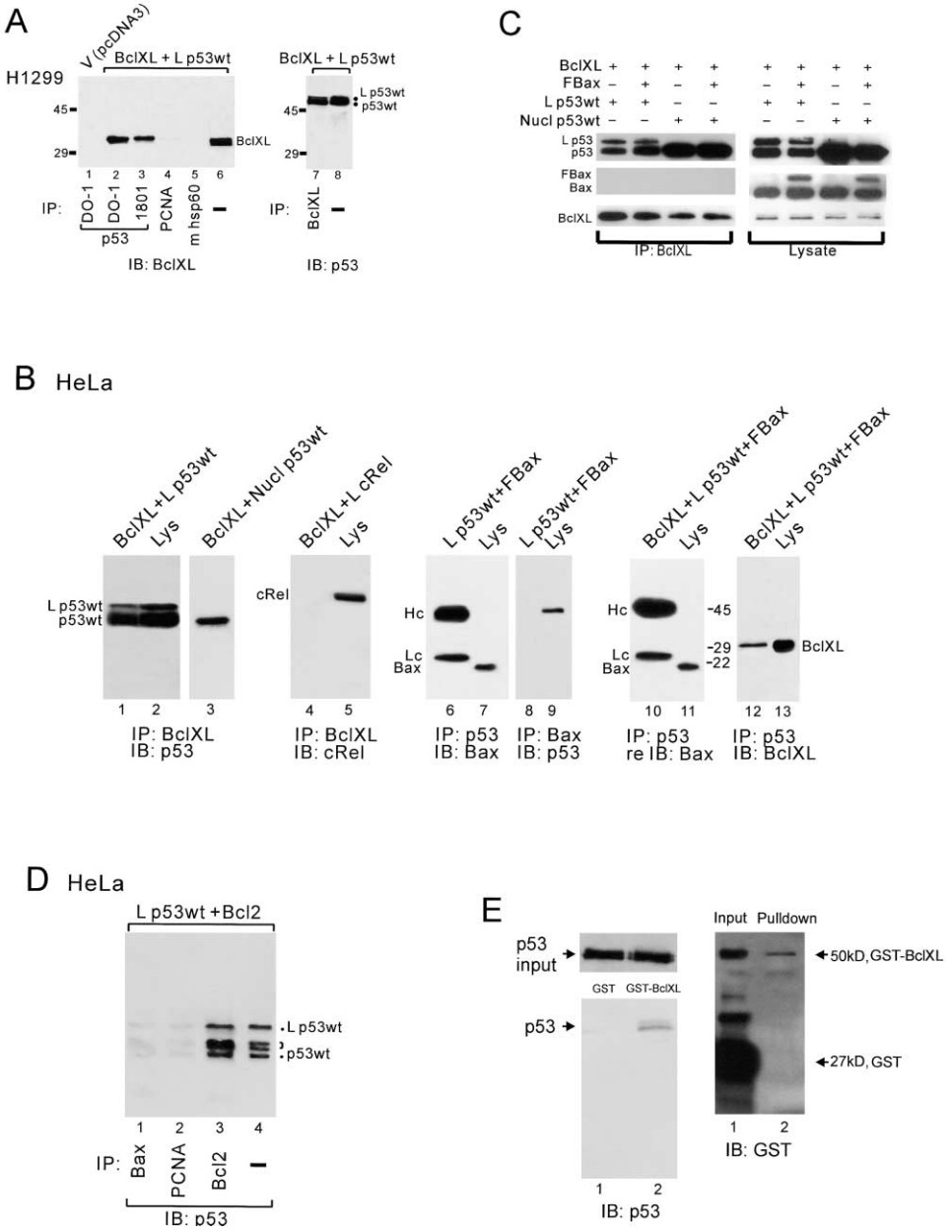

Figure 3. Mitochondrially Targeted and Nuclear Wild-Type p53 Form a Specific Complex with BclXL and Bcl2 in Cells and In Vitro

(A) p53 null H1299 cells, cotransfected with Lp53wt and BclXL or empty vector, were immunoprecipitated with p53 antibodies or irrelevant antibodies and immunoblotted for BclXL. −, lysate only. Lanes 2 and 3 represent 5% and 3% of the IP input. Lane 7 shows immunoprecipitation with α-BclXL followed by p53 blotting.

(B) Targeted and nuclear p53 form a complex with BclXL (lanes 1–3). Lys, lysate only. HeLa cells were cotransfected as indicated. While a small amount of uncleaved Lp53wt fusion is present, the majority of the complex contains free p53, indicating cleavage by mitochondrial endopeptidase and redistribution of p53 to the outer membrane. BclXL does not form a complex with the mitochondrially targeted cRel (LcRel) (lanes 4 and 5). Bax does not form a complex with targeted p53 (lanes 6–11) but a targeted p53/BclXL complex readily forms in the presence of Bax (lanes 12 and 13).

(C) Bax is unable to interfere with the p53/BclXL complex. HeLa cells were either double or triple transfected with the indicated plasmids. Cell lysates were immunoprecipitated with α-BclXL and immunoblotted as indicated. Lanes 5–8, corresponding lysates; FBax indicates Flag-tagged Bax.

(D) Targeted p53 forms a specific complex with Bcl2. HeLa cells cotransfected with Lp53wt and Bcl2 were immunoprecipitated with α-Bcl2 (lane 3) or irrelevant antibodies (lanes 1 and 2) prior to blotting with α-p53.

(E) Direct binding between p53 and BclXL in vitro. (Left) Purified baculoviral p53 was mixed with recombinant GST-BclXL or GST alone. Complexes were captured with Glutathione Sepharose, and bound protein was detected by p53 immunoblot. p53 input is shown on top. (Right) GST-BclXL plus excess free GST (Input) was mixed with purified His-tagged p53. Complexes were pulled down with Nickel-Agarose, and bound protein was detected by GST immunoblot. Lane 2 represents 5% of the input.

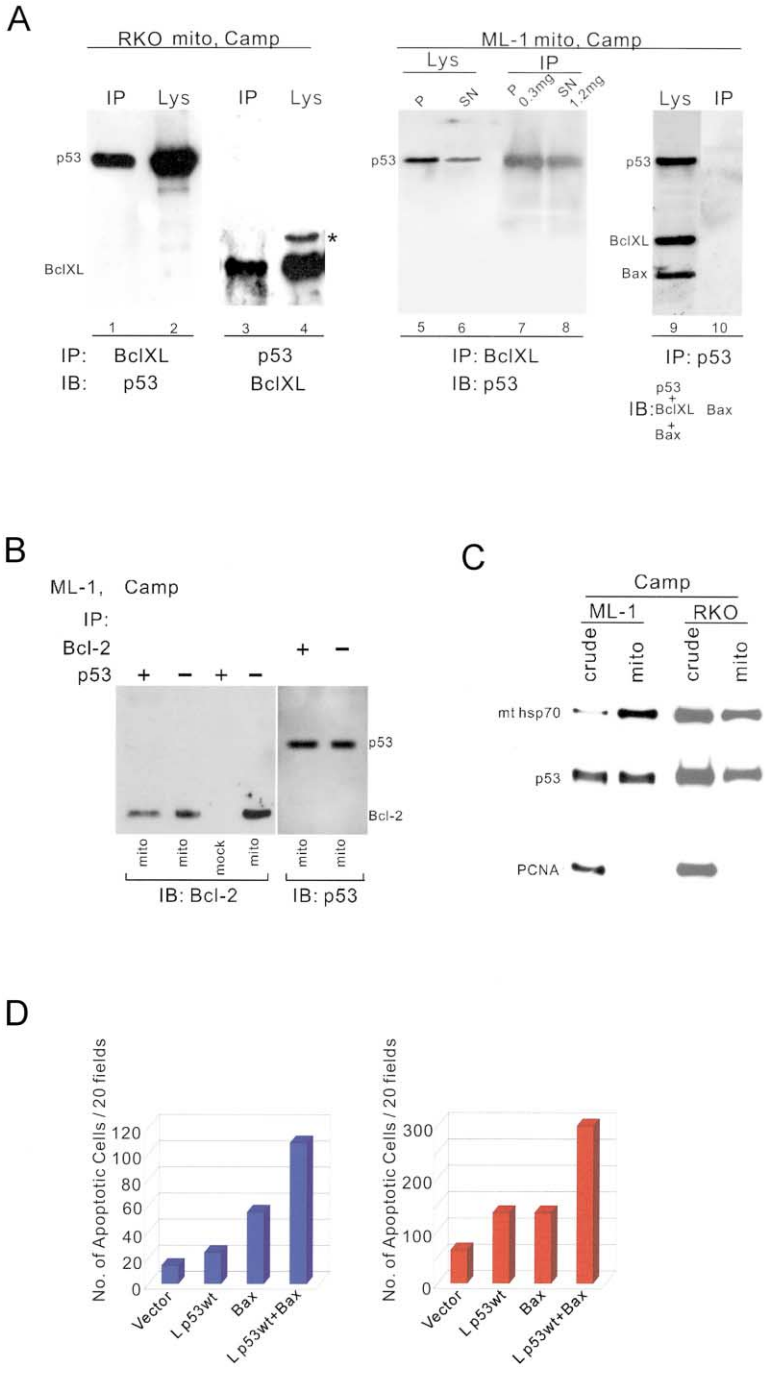

Figure 4. Endogenous Complexes between wtp53 and BclXL or wtp53 and Bcl2 Form in Mitochondria of Stressed Cells

(A and B) wtp53-containing RKO and ML-1 cells were subject to short-term DNA damage (5 μM camptothecin for 5 hr). Extracts from sonicated and solubilized mitochondria were immunoprecipitated followed by blotting with the indicated antibodies. Lys, lysate only. P, mitochondrial pellet; SN, supernatant; mock, contains no extract. * denotes a variable nonspecific band.

(C) Mitochondria used in (A) and (B) were free of nuclear contamination. PCNA, p53, and mthsp70 immunoblots (5 μg per lane).

(D) Targeted wtp53 and Bax cooperate in promoting cell death. HeLa cells were single or double transfected with 300 ng each of the indicated plasmids. After 24 hr, apoptosis in expressing cells was quantitated by Hoechst staining, counting 20 random microscopic fields. Two representative experiments from a total of four are shown.

main (TM) of Bcl2 as a more direct way of p53 targeting, since p53-TM fusions should insert directly into the OMM. Indeed, both N- and C-terminal p53-TM fusions targeted highly efficiently to mitochondria (Figure 5A). And as already seen with Lp53wt, the p53-TM fusion proteins are also defective in transactivation as seen by sensitive reporter assays with the consensus PG13 element and endogenous p53-responsive PUMA and PIG3 promoters (Figure 5B). Importantly, p53-TM fusions also formed a specific complex with BclXL and promoted colony suppression of SaOs2 cells (Figures 5C and 5D). Thus, using two independent ways of bypassing the nucleus, targeting p53 to mitochondria suffices to induce death in p53 null cells. This ability correlates with the formation of mitochondrial p53/BclXL complexes.

Structure/Function Analysis of the p53-BclXL Complex

We next used protein modeling to determine the structural basis for the p53/BclXL complex and predict putative interaction sites between the two proteins. Using the existing crystallographic structures of the human p53 DNA-BD (pdb entry 1TSR) and human BclXL (pdb entry 1LXL) as input into the Global Range Molecular

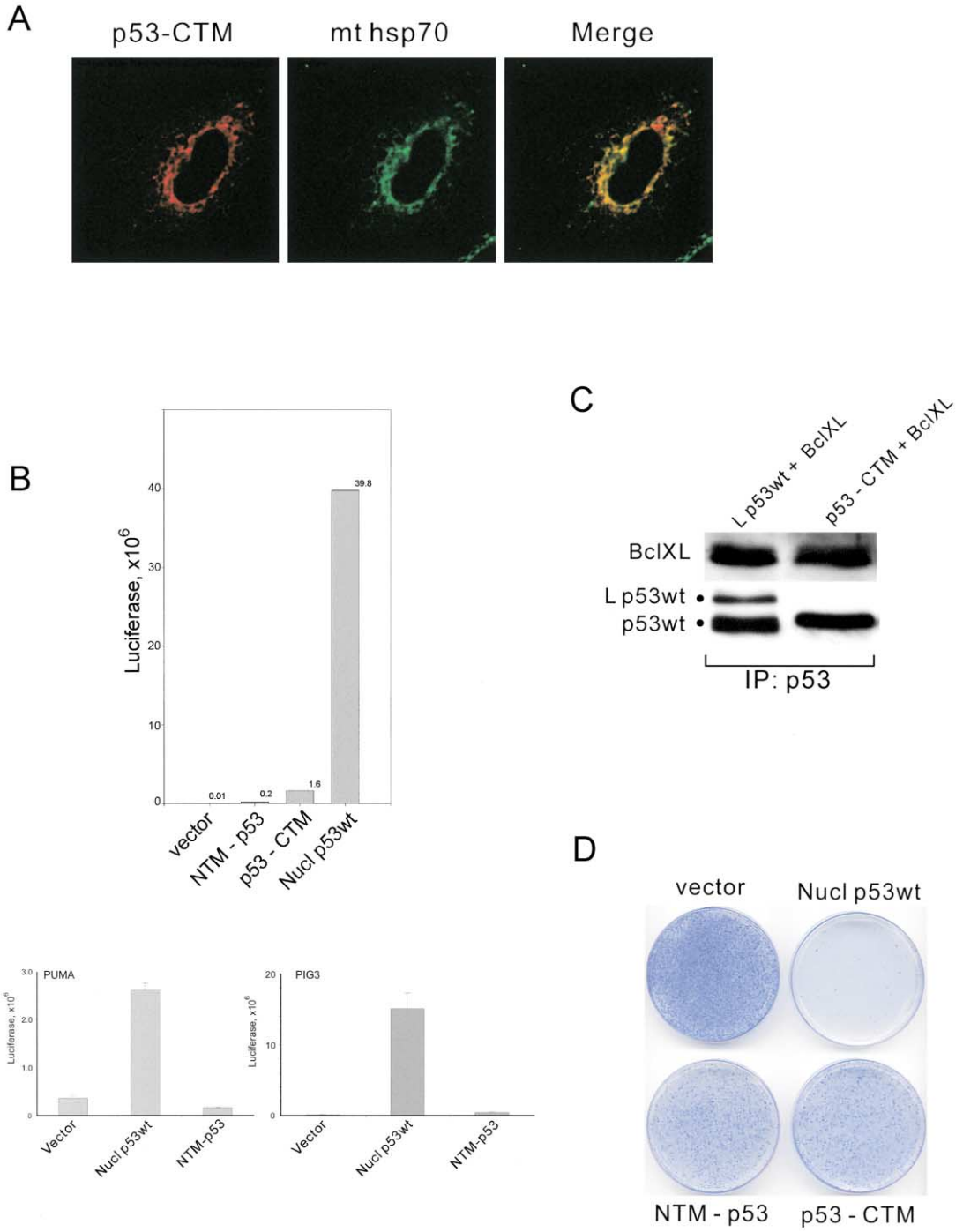

Figure 5. wtp53 Fused to the Transmembrane Domain of Bcl2 Targets to Mitochondria, Lacks Transactivation Function, Forms a Complex with BclXL, and Promotes Growth Suppression

(A) N- and C-terminal fusions between p53 and the transmembrane domain of human Bcl2 (aa 211–239), called NTM-p53 and p53-CTM, colocalize with the mitochondrial marker mt hsp70, without nuclear staining. SaOs2 cells transfected with p53-CTM are shown here.

(B) p53-TM fusions lack transactivation activity. Luciferase reporter assays driven by PG13 consensus response element (top) or the endogenous PIG3 and PUMA promoters (bottom). SaOs2 cells were transfected with 500 ng of each plasmid.

(C) SaOs2 cells transfected with the indicated plasmids were immunoprecipitated for p53 followed by BclXL blotting (top). Equal amounts of immunoprecipitated p53 were loaded (bottom).

(D) Saos2 colony suppression assay after transfection with indicated plasmids. Crystal violet staining after 12 days of G418 selection.

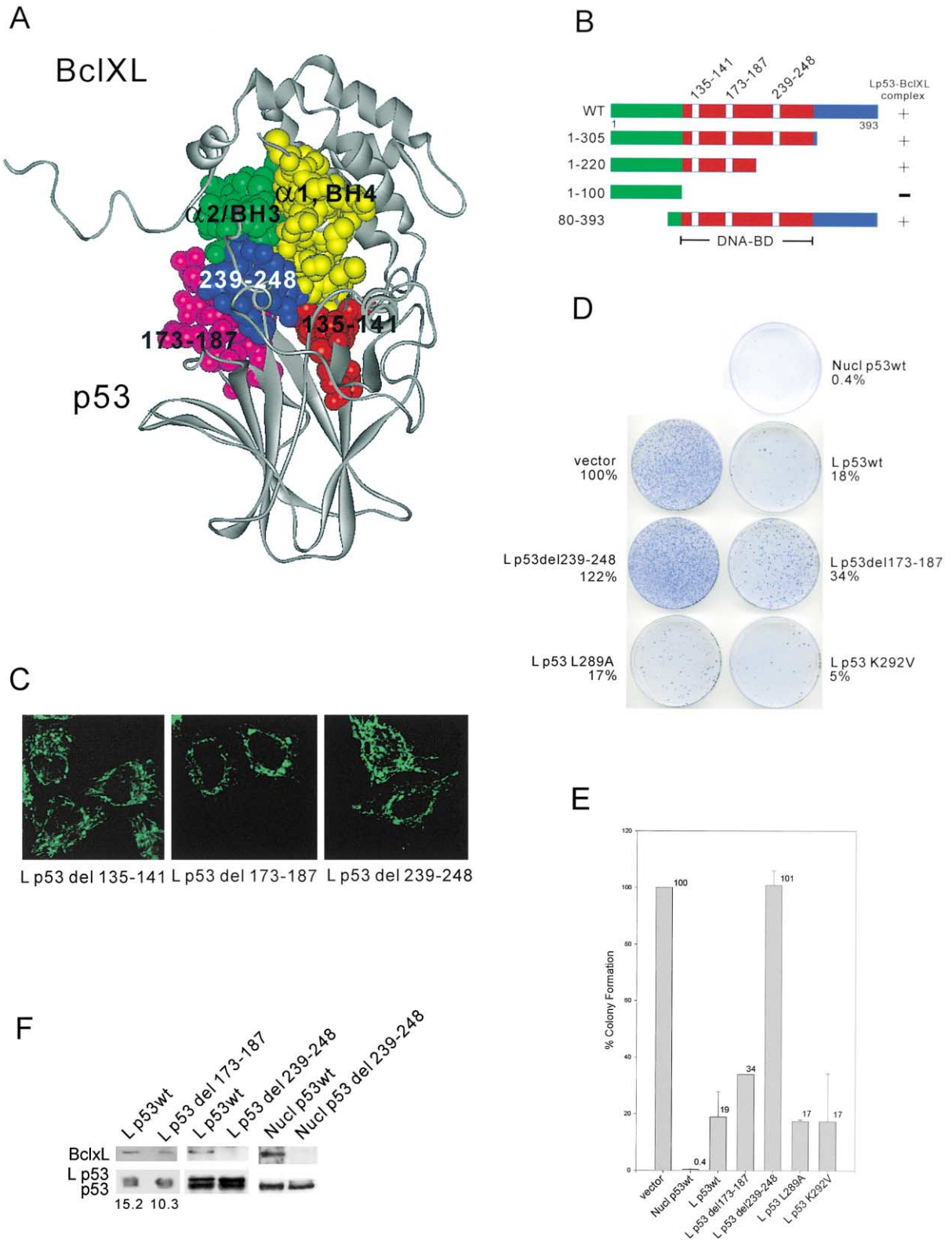

Figure 6. Structure/Function Analysis of the p53-BclXL Complex

(A) Space filling model of the complex. The p53 DNA binding domain contacts BclXL. The protruding blue region of human p53 spanning residues 239–248, flanked by regions 135–141 (red) and 173–187 (magenta), interact with a groove formed by the α1/BH4 and part of the α2/BH3 domains of human BclXL.

(B) Mapping the BclXL binding domain on p53. H1299 cells cotransfected with BclXL and the indicated p53 mutants were immunoprecipitated and assayed for complex formation with BclXL. DNA-BD, p53 DNA binding domain. See also Supplemental data at http://www.molecule.org/cgi/content/full/11/3/577/DC1.

Matching Program (Vakser and Nikiforovich, 1995), we employed a classic protein folding algorithm that we expanded by integrating quantitative local context descriptors for each amino acid position within the polypeptide sequence of each protein. This allows the computation of contextual similarity surfaces of two interaction partners (detailed description of the method will be published elsewhere). For validation, our algorithm correctly predicted the structure and interaction surfaces of a crystallographically solved complex between the p53 DNA binding domain and 53BP2 (data not shown) (pdb entry 1YCS; Gorina and Pavletich, 1996), while it did not predict the existence of a p53/Bax complex, consistent with our experimental data. We computed about 500 possible structures for a p53/BclXL complex, but only the structure in Figure 6A satisfies the constraints given by the contextual similarity analysis (see also Supplemental Figure S1 at http://www.molecule.org/cgi/content/full/11/3/577/DC1). The contact surface involves the p53 DNA binding domain, interacting with the α1/BH4 and partial α2/BH3 domains of BclXL. The major contact site on p53, comprised of residues 239–248 (part of the L3 loop), is the most protruding and centrally located. This domain is flanked by two lateral domains on either side, contributed by residues 135–141 (L1 loop) and residues 173–187 (part of the L2 loop and H1 helix). Using coimmunoprecipitation assays on a series of N- and C-terminal truncations of Lp53wt, we mapped the BclXL binding domain of p53 to its DNA binding domain (Figure 6B). Lp53(1–305), Lp53(1–220), and Lp53(80–393) were able to bind to BclXL, while Lp53(1–100), which is missing the contact sites, had lost its binding. Together, these data implicate the p53 core domain to interact with BclXL. To determine the importance of BclXL binding for mitochondrial p53 function, we deleted each of the contact regions from Lp53wt and tested them for loss of mitochondrial killing activity. All mutants targeted exclusively to mitochondria (Figure 6C). Deleting amino acids 239–248 from targeted p53 completely abrogated its apoptotic and colony suppression activity in Saos2 and HeLa cells (Figures 6D and 6E and Supplemental Figure S2 [http://www.molecule.org/cgi/content/full/11/3/577/DC1]). Importantly, loss of apoptotic ability of the 239–248 mutant correlated with loss of its BclXL binding ability, as shown by quantitative immunoprecipitations (Figure 6F). While targeted and nuclear wtp53 readily formed a BclXL complex (lanes 1, 3, and 5), targeted and nuclear versions of the 239–248 mutant exhibited a loss of BclXL binding (lanes 4 and 6). Deleting the flanking regions 135–141 and 173–187 caused a partial phenotype with respect to colony suppression, apoptosis, and BclXL binding (Figures 6D–6F and Supplemental Figure S2). Together, these data suggest good structure-function correlation between the ability of p53 to form BclXL complexes and its ability to induce cell death via the mitochondrial pathway.

Naturally Occurring Mutations in Human Tumors Select against the Transcriptional *and* Mitochondrial Apoptotic Activity of p53

Our model implies that the DNA binding domain of p53 is a dual-function domain, mediating both the transactivation and the mitochondrial proapoptotic function. This leads to the prediction that missense mutations in this region abrogate both functions. During malignant transformation of human tumors, p53 mutations are selected for loss of their apoptotic and tumor suppressor ability, which coincides with loss of their transactivation function (Hollstein et al., 1999). Do tumor-derived p53 mutants concomitantly lose the ability to bind to BclXL? We examined four randomly chosen tumor-derived breast cancer cell lines with mutant p53 and LOH of the wt alleles. SKBr3 harbors R175H, T47D harbors L194F, MDA 468 harbors R273H, and MDA 231 harbors R280K. Together, these four mutations represent 13% of all p53 mutations found in over 16,000 human tumors (IARC p53 database [http://www.iarc.fr/p53/Index.html]). The R175H mutant is the prototype of a structural mutant due to unfolding of the β sandwich scaffold of the DNA-BD. The R273H mutant is a classic DNA contact mutant and both are hotspots in human cancers. Arg280 is part of the H2 helix and makes direct contact with the major groove. Leu194 is immediately adjacent to the hydrophobic core of the β sandwich (Cho et al., 1994).

Using careful quantitative coimmunoprecipitations, we compared the amount of endogenous p53/BclXL complexes in wtp53 harboring RKO cells with those of mutant p53 cells. Due to lack of HDM2 induction, mutant cells have high total levels of p53. Of note, proportional to their abnormally stabilized p53, all four lines constitutively harbor readily detectable levels of mutant p53 at the mitochondria in the absence of a death stimulus (Figure 7A). This is in sharp contrast to wtp53 cells, whose mitochondrial p53 translocation depends on induction by death stimuli. However, despite constitutively high levels of mutant p53 at the mitochondria, three of the four cell lines (SKBr3, T47D, and MDA 468) reproducibly showed no detectable endogenous p53/BclXL complexes, regardless of whether cells were subjected to prior DNA damage or not (Figures 7C and 7D). The fourth line (MDA 231) showed a greatly reduced amount of p53/BclXL complex (Figure 7D). The absence of detectable mutant p53/BclXL complexes was in stark contrast to readily detectable endogenous wtp53/BclXL complexes from camptothecin-treated RKO cells (Figure 7C, lane 1) and cotransfected Hela cells (Figure 7D, lanes 1 and 2). Of note, the endogenous BclXL levels of

(C–E) Deletion of residues 239–248 of p53 abrogates its mitochondrial killing activity. (C) Immunofluorescence of HeLa cells transfected with the indicated targeted p53 contact mutants. Lp53 L289A, Lp53 K292V, and LcRel also show exclusive mitochondrial localization (see Supplemental Figure S3 at http://www.molecule.org/cgi/content/full/11/3/577/DC1). (D) Saos2 colony formation assay after transfection with the indicated targeted p53 binding mutants. Vector is set as 100% (see Supplemental Figure S3). (E) Three independent experiments +/− SD.
(F) Deleting the BclXL contact regions of p53 decreases or abolishes its affinity to BclXL. Transfected H1299 cells were immunoprecipitated for p53 and then blotted for associated BclXL. (Bottom) Reblotting with α-p53 confirms equal input of precipitated p53. Numbers indicate density ratios of BclXL.

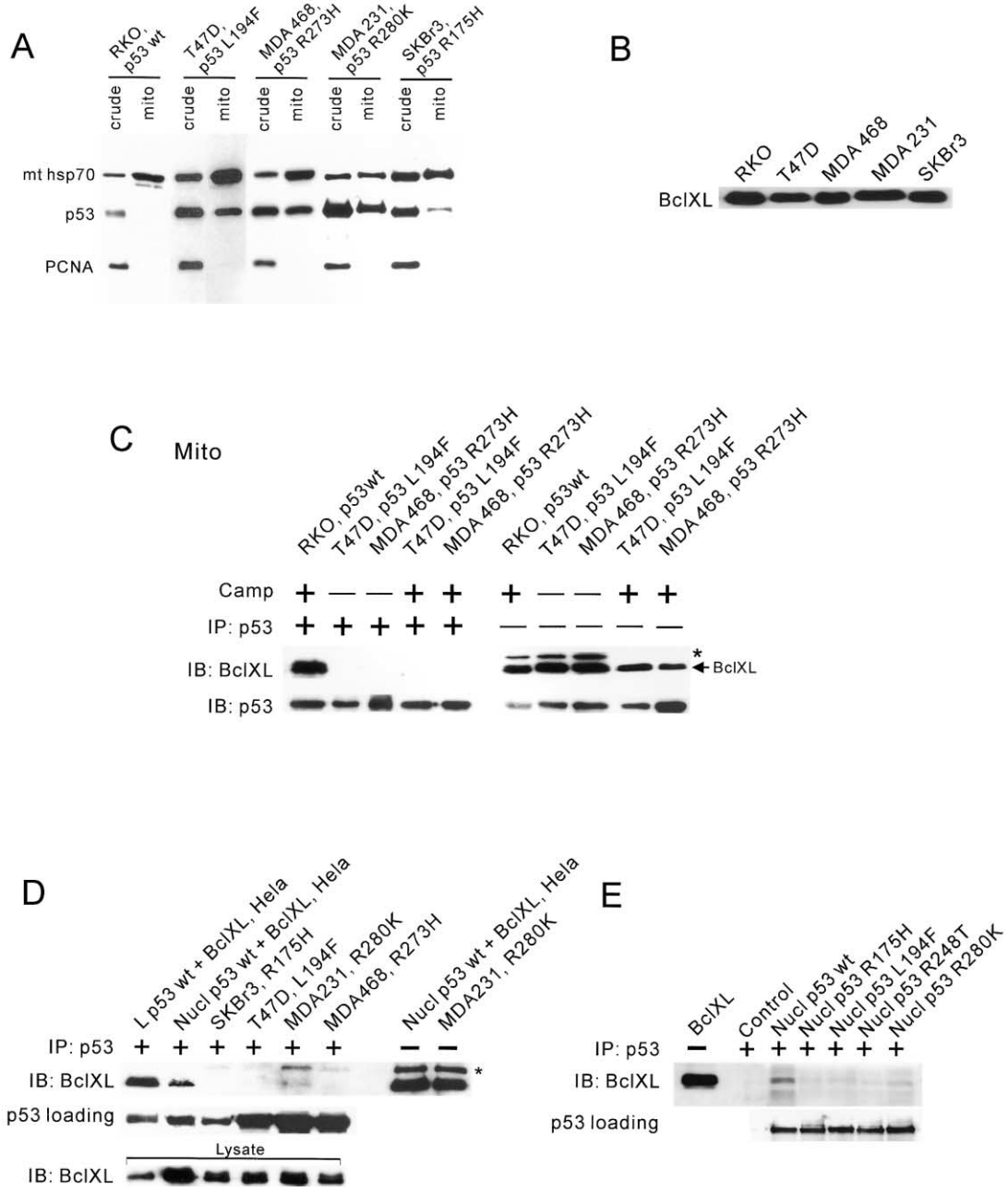

Figure 7. Endogenous Tumor-Derived p53 Mutants Are Deficient in BclXL Complex Formation

(A) In contrast to wtp53, mutant p53 is constitutively present at mitochondria. Immunoblot of crude cell lysates and mitochondria from wtp53 RKO cells and four unstressed mutant breast cancer lines.

(B) Endogenous BclXL levels of wtp53- and mutant p53-harboring cells are comparable. Immunoblot with α-BclXL (10 μg per lane in [A] and [B]).

(C) Isolated mitochondria from Camptothecin-treated wtp53 RKO and mutant p53 breast cancer cells with or without prior treatment were subject to p53 immunoprecipitation and then blotted for associated BclXL. Reblotting with α-p53 confirms comparable loading of precipitated p53. Lanes 6–10, lysates only.

(D) Total cell lysates from breast cancer (lanes 3–6) or HeLa cells cotransfected with BclXL and Lwtp53 (lane 1) or nuclear wtp53 (lane 2) were immunoprecipitated with α-p53 and blotted for BclXL as in (C). Reblotting with α-p53 (middle) confirms similar p53 loading. Lanes 7 and 8 and bottom, lysates only. * denotes a variable nonspecific band.

(E) p53 null H1299 cells were transfected with vector alone (control), or plasmids for nuclear wtp53 or tumor-derived point mutants, followed by coimmunoprecipitation for p53/BclXL interaction as in (C) and (D).

RKO and the mutant cell lines were comparable (Figure 7B). This result was confirmed in an *isogenic* system, using p53 null H1299 cells transfected with plasmids for tumor-derived point mutants. All four p53 mutants showed a greatly decreased ability to form BclXL complexes compared to wtp53 (Figure 7E). Together, these data are very compelling, since they strongly argue for an in vivo role of mitochondrial p53 in human tumors.

It further suggests that tumorigenic mutations that are selected during human tumor formation might represent double-hit mutations by abrogating both the transcriptional and the mitochondrial apoptotic activity of p53.

Purified p53 Protein Triggers the Rapid Release of Cytochrome C from Isolated Mitochondria

What is the functional basis of the proapoptotic action of mitochondrial p53? Of note, death-stimulus-induced mitochondrial translocation of p53 precedes the release of cytochrome c (Marchenko et al., 2000). To test whether cytochrome c release is a *direct* effect of wtp53 translocation, we asked whether baculoviral wtp53 alone was sufficient to trigger cytochrome c release from freshly isolated mouse liver mitochondria. This classic assay was used to establish the membrane-permeabilizing effect of Bax and Bak proteins (Jurgensmeier et al., 1998; Eskes et al., 1998). The purity of all our p53 preparations was verified by silver gels showing a single band of 53 kDa (Figure 8A). Strikingly, incubation with mouse wtp53 triggered the release of over 90% of mitochondrial cytochrome c within 30 min, similar to $CaCl_2$, a known permeabilizer and PTP pore opener (Eskes et al., 1998), while buffer alone released $<5\%$ (Figure 8B). This effect was due to added p53, since endogenous p53 levels of unstressed mitochondria were undetectable (Figure 8D, lane 1), and it was dose dependent with significant release with 400 nM and maximum release with 1 μM of wtp53 (Figure 8C, lanes 1–4). In contrast, a C-terminal fragment of p53 (aa 315–390) failed to induce release (Figure 8C, lanes 5–8). Moreover, p53-induced cytochrome c release is fast. Within 5 min after adding p53, 69% of the total cytochrome c release has already occurred and is almost complete at 30 min (Figure 8D, lanes 4, 6, 8, and 10). Importantly, the amount of mitochondria-associated p53 remained constant between 0 and 60 min, suggesting that p53 binding to mitochondria is a very rapid, saturable process. Identical results were obtained with human wtp53 from baculoviral and bacterial sources.

What is the mechanism by which p53 triggers cytochrome c release? Is there a direct link between p53/BclXL complex formation and cytochrome c release? To test this notion, we looked for complexes in pellets of mitochondria *after* cytochrome c release had occurred (after 30 min incubation with 400 nM wtp53). Indeed, in these post-release mitochondria, p53/BclXL complexes were clearly detected (Figure 8E, lane 1). This supports a mechanism where p53 directly induces permeabilization of the outer mitochondrial membrane by forming inhibitory complexes with BclXL. Furthermore, since p53 is a direct inducer of cytochrome c release and of mitochondrial dysfunction, p53 might also indirectly activate the ultimate effectors for cytochrome c release—Bak and Bax proteins—by inducing their conformational change and intramembraneous oligomerization. To test this, we examined whether p53 induces Bak oligomerization (mouse liver mitochondria are poor in Bax). Indeed, using the chemical crosslinker BS3, purified wtp53, when added to freshly isolated nascent mitochondria, readily induced crosslinked Bak multimers, consistent with trimers (72 kDa) and tetramers (96 kDa) (Figure 8F, lane 2). This p53 behavior is similar to the prototypical BH3-only protein tBID which translocates to mitochondria upon a death stimulus to induce Bak oligomerization (Figure 8F, lane 1). Moreover, since overexpression of BclXL and Bcl2 completely block p53-dependent apoptosis in vivo (Schuler and Green, 2001), it predicts that excess BclXL also prevents p53-induced cytochrome c release in vitro. To address this, we performed BclXL competition experiments. Indeed, the effectiveness of p53 in inducing cytochrome c release is inhibited in a dose-dependent fashion by adding increasing amounts of excess GST-BclXL (Figure 8G), indicating that p53 and antiapoptotic BclXL proteins are in a rheostat-like relationship. Together, these data demonstrate that p53 itself is able to directly permeabilize the OMM and trigger the release of proapoptotic activators. It does so by engaging in inhibitory complexes with protective Bcl2/XL, thereby indirectly activating proapoptotic BH123 proteins like Bak.

The most persuasive evidence for the physiologic importance of the mitochondrial p53 pathway would come from the behavior of mutant p53 proteins. Is there a direct functional link between the failure of p53 mutants to form BclXL complexes (Figures 7C–7E) and a failure to release cytochrome c in vitro? Indeed, in contrast to wtp53 that readily induces release, tumor-derived mutant p53 proteins are defective in permeabilizing the outer membrane. The hotspot mutant R175H has completely lost the ability to release cytochrome c, while the hotspot mutant R273H is severely suppressed in this activity (Figure 8H). Thus, this direct link supports the hypothesis that tumors select against both the nuclear and mitochondrial apoptotic function of p53. Moreover, it shows that the interaction with BclXL is required for p53-mediated cytochrome c release.

Discussion

The present data reveal an extranuclear death function of p53 and show that this function is critically involved in mediating the proapoptotic action of p53 at the mitochondria. We show that p53 protein can directly induce permeabilization of the outer mitochondrial membrane by forming inhibitory complexes with protective Bcl proteins, resulting in cytochrome c release. p53 binds to BclXL via its DNA binding domain. This mitochondrial action might be derailed in tumors since at least some p53 mutants lose the ability to interact with BclXL and promote cytochrome c release. Thus, tumor-derived mutations might represent double-hits by concomitantly abrogating the transcriptional and mitochondrial apoptotic activity of p53.

Functional parallels between p53 and other proapoptotic proteins appear to be emerging. p53, Noxa, Puma, Bim, and Bad all rapidly translocate to mitochondria upon a death stimulus, bind and inhibit the protective BclXL and Bcl2 proteins, and induce OMM permeabilization, leading to cytochrome c release and caspase activation. For both p53 and the BH3 proteins, complex formation with BclXL/2 is critical for apoptogenicity, since interference with binding blocks their mitochondrial killing activity (our data; Cheng et al., 2001; Oda et al., 2000; Nakano and Vousden, 2001; Yu et al., 2001). Other proapoptotic proteins such as Siva-1 and

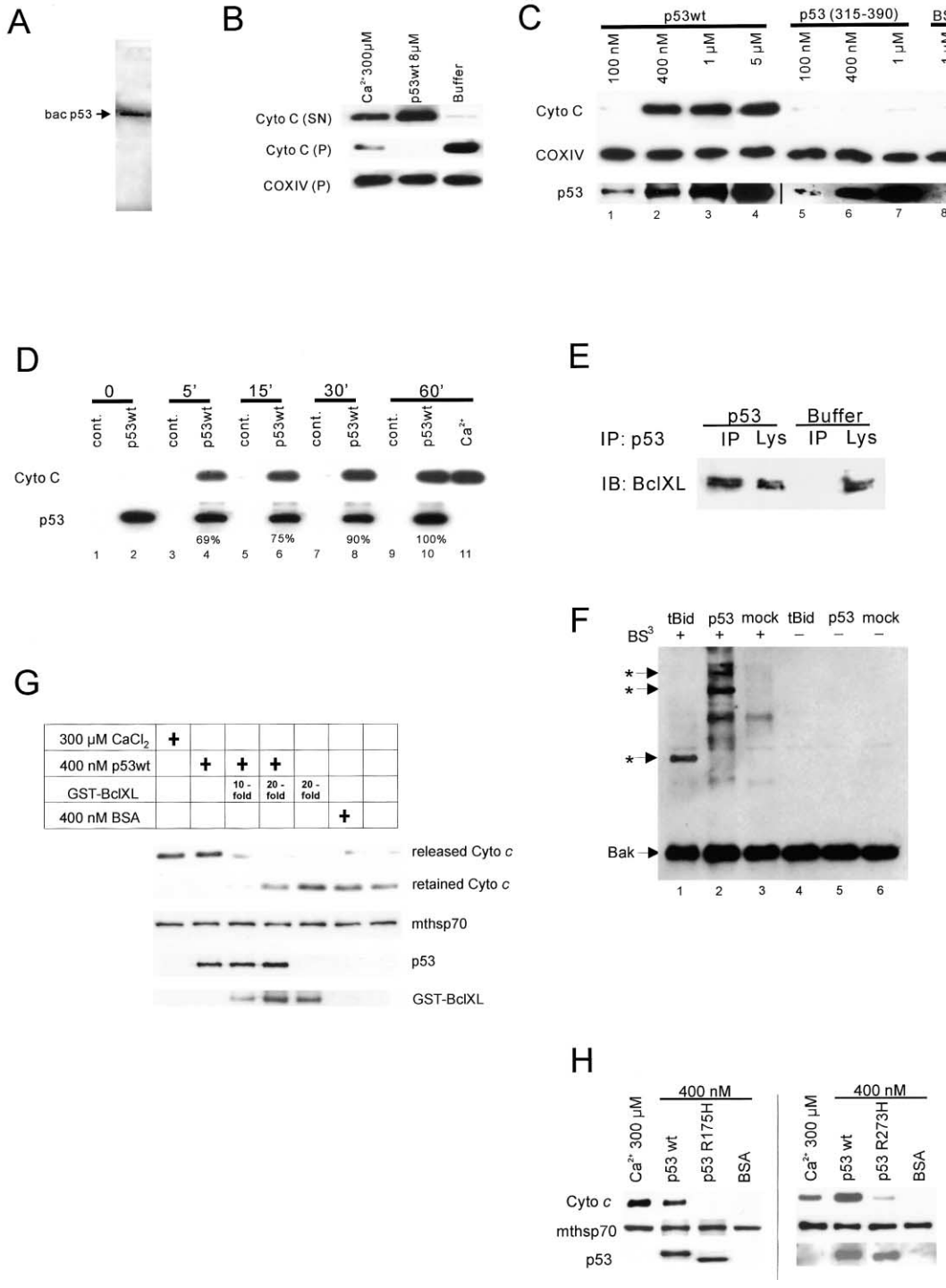

Figure 8. Recombinant p53 Triggers Rapid Release of Cytochrome C from Isolated Mouse Liver Mitochondria

(A) Purity of baculoviral p53 used in cytochrome c release assays. Silver gel (1.2 μg).

(B) Mitochondria were incubated for 30 min with $CaCl_2$, wtp53, or buffer. Released and retained cytochrome c was determined by blotting 5 μg each of mitochondrial supernatant (SN) and pellet (P) with α-Cyto C. Pellet membrane was reblotted for COX IV as loading control.

(C) Dose response curve of p53-induced cytochrome c release. Mitochondria were incubated with increasing concentrations of wtp53, C-terminal p53 peptide, or BSA. Supernatants were immunoblotted with α-cytochrome c. Pellets were blotted with α-COXIV as loading control and reblotted to confirm input of wtp53 and p53 peptide.

(D) Kinetics of p53-induced cytochrome c release. Mitochondria were incubated for 0–60 min with either 1 μM BSA (cont.) or 400 nM wtp53. Lane 11 contains 100 μM $CaCl_2$. Supernatants were immunoblotted for cytochrome c and pellets for input p53.

(E) Post-release mitochondria contain a p53/BclXL complex. After 30 min incubation with 400 nM wtp53 or buffer, mitochondrial pellets (50 μg) were immunoprecipitated followed by blotting with the indicated antibodies. Lys, lysate only. Lane 1 represents 15% of the input.

(F) p53 induces oligomerization of BAK. Mitochondria were incubated with 1 μM GST-tBid, 400 nM wtp53, or buffer in the presence or absence

p53AIP1, which like p53 lack a BH3 domain, also bind and inactivate BclXL (Xue et al., 2002; Matsuda et al., 2002). While BH3-only proteins bind BclXL/2 through their BH3 domain, SIVA-1 binds through a unique amphipathic helix (Xue et al., 2002) and p53 binds through its central core effector domain (our data). Our finding of the ability of excess BclXL to block p53-mediated cytochrome c release in vitro parallels that seen with Bax and tBid (Jurgensmeier et al., 1998; Desagher et al., 1999). Also, Puma- and Siva-1-mediated apoptosis is suppressed by excess BclXL (Nakano and Vousden, 2001; Xue et al., 2002).

In summary, our study provides a mechanistic basis for transcription-independent apoptosis by p53 and opens a new avenue toward comprehensive understanding of p53 function. We propose that p53 exerts a rapid and direct proapoptotic role at the mitochondria, thereby jump-starting and amplifying its transcription-based apoptotic action that requires more time to take effect. Given its implication in a broad spectrum of cell types and death signals and the central role of mitochondria in p53-mediated apoptosis, this pathway could enhance many types of p53-mediated killing. A complete analysis with respect to tissue types and gamut of stress signals will further delineate the scope of this pathway in p53 stress responses. Another future question is the relative contributions of the transcriptional and mitochondrial pathways to tumor suppression in vivo. Based on the pleiotropic p53 function, it might well be that individual effector pathways are necessary but not sufficient to execute the full scale of the p53 death and suppressor program.

Experimental Procedures

Cell Culture

Cells were grown in RPMI 1640 (ML-1) or DMEM (all others), plus 10% FBS. Camptothecin (Sigma) stress was always 5 μM for 5 hr.

Mitochondrial Fractionation

Mitochondria were prepared by sucrose density gradients (Marchenko et al., 2000). Thymocytes of 4- to 6-week-old C57BL/6 females were isolated within 5 min of sacrifice, pulse treated with 10 Gy, and incubated for 1 hr at 37°C prior to mitochondrial isolation.

Immunoblots and Coimmunoprecipitation

Equal total protein of mitochondrial and crude cell lysates were immunoblotted with the following antibodies: monoclonal 1801, 240 and DO-1 (Santa Cruz Biotechnology), or polyclonal CM-1 (Vector) for human p53; UM-1 for mouse p53 (raised against recombinant mouse wtp53); mt hsp60 and mt hsp70 (Affinity Bioreagents); PCNA, GST, and cRel (Santa Cruz), cytochrome c (Pharmingen), and cytochrome oxidase IV (Molecular Probes); polyclonal BclXL (S18 and L19; Santa Cruz), Bcl2 (Transduction Labs), Bax (Neomarker), Noxa (Imgenex), Bak (Upstate Biotechnology), and Flag and rabbit IgG (Sigma). For endogenous complexes, mitochondrial lysates (1 mg) from Camp-treated ML-1 or RKO cells were immunoprecipitated with 1 μg antibody and immunoblotted. For exogenous complexes, whole-cell lysates (1 mg) of transfected cells were used. For quantitative immunoprecipitations in Figure 7, 200 μg of mitochondrial (C) or 1 mg of whole-cell (D) lysates were incubated with 20 μl of DO-1 plus 1801 Sepharose beads for 2 hr. Beads were washed three times with SNNTE plus 2 × RIPA (50 mM Tris, 150 mM NaCl, 1% Triton X-100, 0.1% SDS, 1% NaDeoxycholate [pH 7.4]) and subjected to an initial Western blot for quantitation. Loading of the definitive blot was then normalized for equal amounts of immuneprecipitated p53 and blotted for BclXL. For pull-down experiments, purified human full-length GST-BclXL (Chittenden et al., 1995) and/or free GST were incubated with purified baculoviral His-tagged wtp53, washed, and pulled down with either glutathione sepharose or Ni-NTA Agarose beads. Luciferase reporter assays were performed with PG13-Luc, PUMA-Luc (Yu et al., 2001), and PIG3-Luc (Contente et al., 2002) reporters. All values were normalized for Renilla activity.

Apoptosis and Colony Suppression Assays

TUNEL assays were performed as described (Marchenko et al., 2000). For colony suppression, SaOs2 cells (1×10^3) in 100 mm plates were transfected with 300 ng of the indicated plasmids. 48 hr later, cells were placed under G418 selection (500 μg/ml) for 12–18 days, fixed, and stained with crystal violet. Foci were quantitated via integral optical plate density (BioRad, Laser Pix Software), setting vector as 100%.

Plasmid Constructions

All deletion and point mutants were generated by PCR into a pcDNA3-based plasmid encoding a mitochondrial import leader and cleavage site for mitochondrial endopeptidase, fused to the N terminus of wt p53 (Marchenko et al., 2000). For mitochondrial p53 targeting via the transmembrane (TM) domain of Bcl2, N- and C-terminal fusions of wtp53 and TM domain (aa 211–239) of human Bcl2 were generated by PCR: NTMp53wt (TMp53(3–393)) and p53wtCTM (p53(1–392)TM). Expression plasmids of human Bcl2, BclXL, and Bax (Chittenden et al., 1995) and LcRel were described (Marchenko et al., 2000). All constructs were sequence confirmed and shown to target to mitochondria by colocalization by immunofluorescence.

Cytochrome C Release

Freshly harvested livers of 10-week-old C57BL/6 mice were used for mitochondrial isolation (Eskes et al., 1998). His-tagged baculoviral human and mouse mutant and wild-type p53 or C-terminal fragment were purified over Ni-NTA agarose, followed by heparin and MonoQ/FPLC columns. Immunoaffinity-purified baculoviral p53 R175H protein was a gift of C. Prives. p53 and BSA (Sigma) were dialyzed against KCl buffer (15 mM HEPES/NaOH, 125 mM KCl, 4 mM $MgCl_2$, 5 mM Na_2HPO_4, 0.5 mM EGTA, 5 μM Rotenon (Sigma), 5 mM succinate [pH 7.4]). Mitochondria (70 μg protein) were incubated with proteins for 30 min at 30°C in 200 μl KCl buffer, then centrifuged at 13,000 g for 10 min at 4°C. Mitochondrial pellets (5 μg) and corresponding supernatants were immunoblotted for cytochrome c and cytochrome oxidase IV (COXIV) antibodies to verify equal loading. For crosslinking experiments, 70 μg of freshly isolated liver mitochondria was incubated with 400 nM wtp53 or 1 μM purified GST-tBid or buffer (mock) in the presence or absence of 2 mM crosslinker BS^3 (Bissulfosuccinitidyl suberate; Pierce) for 30 min at room temperature.

---

of 2 mM crosslinker BS^3 for 30 min. Crosslinked Bak species were detected by Bak immunoblot. * indicates Bak complexes consistent with dimers, trimers, and tetramers. While endogenous tBid and Bim induce trimeric and tetrameric Bak complexes, recombinant GST-tBid mainly generates Bak dimers (Wei et al., 2000; Cheng et al., 2001).

(G) p53-induced cytochrome c release in vitro is inhibited by excess BclXL. Cytochrome c release assay as in (C), but where indicated 10- to 20-fold molar excess of GST-BclXL was added at the start of the reaction. Released and retained cytochrome c was determined by blotting 5 μg of mitochondrial supernatant and pellet each with α-Cyto C. Pellet membrane was reblotted for mthsp70 (loading control) and for p53 and GST-BclXL to show input.

(H) Tumor-derived hotspot mutant p53 proteins are defective in inducing cytochrome c release. Cytochrome c release assay as above with baculoviral wt or mutant p53 (400 nM). Calcium and BSA (400 nM) are used as controls. Equal input of p53 and mitochondria is shown by reblotting the post-release pellets with α-p53 and α-mthsp70 antibodies.

Acknowledgments

We thank A. Sidorenko for technical assistance. This work was supported by grants from the NIH/NCI and the American Cancer Society.

Received: June 6, 2002
Revised: January 13, 2003
Published online: January 27, 2003

References

Attardi, L.D., Reczek, E.E., Cosmas, C., Demicco, E.G., McCurrach, M.E., Lowe, S.W., and Jacks, T. (2000). PERP, an apoptosis-associated target of p53, is a novel member of the PMP-22/gas3 family. Genes Dev. *14*, 704–718.

Caelles, C., Helmberg, A., and Karin, M. (1994). P53-dependent apoptosis in the absence of transcriptional activation of p53-target genes. Nature *370*, 220–223.

Chen, X., Ko, L.J., Jayaraman, L., and Prives, C. (1996). P53 levels, functional domains, and DNA damage determine the extent of the apoptotic response of tumor cells. Genes Dev. *10*, 2438–2451.

Cheng, E.H., Wei, M.C., Weiler, S., Flavell, R.A., Mak, T.W., Lindsten, T., and Korsmeyer, S.J. (2001). BCL-2, BCL-X(L) sequester BH3 domain-only molecules preventing BAX- and BAK-mediated mitochondrial apoptosis. Mol. Cell *8*, 705–711.

Chittenden, T., Flemington, C., Houghton, A.B., Ebb, R.G., Gallo, G.J., Elangovan, B., Chinnadurai, G., and Lutz, R.J. (1995). A conserved domain in Bak, distinct from BH1 and BH2, mediates cell death and protein binding functions. EMBO J. *14*, 5589–5596.

Cho, Y., Gorina, S., Jeffrey, P.D., and Pavletich, N.P. (1994). Crystal structure of a p53 tumor suppressor-DNA complex: understanding tumorigenic mutations. Science *265*, 346–355.

Contente, A., Dittmer, A., Koch, M.C., Roth, J., and Dobbelstein, M. (2002). A polymorphic microsatellite that mediates induction of PIG3 by p53. Nat. Genet. *30*, 315–320.

Desagher, S., Osen-Sand, A., Nichols, A., Eskes, R., Montessuit, S., Lauper, S., Maundrell, K., Antonsson, B., Martinou, J.C. (1999). Bid-induced conformational change of Bax is responsible for mitochondrial cytochrome c release during apoptosis. J. Cell Biol. *144*, 891–901.

Ding, H.F., Lin, Y.L., McGill, G., Juo, P., Zhu, H., Blenis, J., Yuan, J., and Fisher, D.E. (2000). Essential role for caspase-8 in transcription-independent apoptosis triggered by p53. J. Biol. Chem. *275*, 38905–38911.

Eskes, R., Antonsson, B., Osen-Sand, A., Montessuit, S., Richter, C., Sadoul, R., Mazzei, G., Nichols, A., and Martinou, J.C. (1998). Bax-induced cytochrome C release from mitochondria is independent of the permeability transition pore but highly dependent on Mg2+ ions. J. Cell Biol. *143*, 217–224.

Eskes, R., Desagher, S., Antonsson, B., and Martinou, J.C. (2000). Bid induces the oligomerization and insertion of Bax into the outer mitochondrial membrane. Mol. Cell. Biol. *20*, 929–935.

Friedman, P.N., Chen, X., Bargonetti, J., and Prives, C. (1993). The p53 protein is an unusually shaped tetramer that binds directly to DNA. Proc. Natl. Acad. Sci. USA *90*, 3319–3323.

Gao, C., and Tsuchida, N. (1999). Activation of caspases in p53-induced transactivation-independent apoptosis. Jpn. J. Cancer Res. *90*, 180–187.

Gorina, S., and Pavletich, N.P. (1996). Structure of the p53 tumor suppressor bound to the ankyrin and SH3 domains of 53BP2. Science *274*, 1001–1005.

Green, D.R., and Evan, G.I. (2002). A matter of life and death. Cancer Cell *1*, 19–30.

Haupt, Y., Rowan, S., Shaulian, E., Vousden, K.H., and Oren, M. (1995). Induction of apoptosis in HeLa cells by trans-activation-deficient p53. Genes Dev. *9*, 2170–2183.

Huang, D.C., and Strasser, A. (2000). BH3-only proteins-essential initiators of apoptotic cell death. Cell *103*, 839–842.

Hollstein, M., Hergenhahn, M., Yang, Q., Bartsch, H., Wang, Z.Q., and Hainaut, P. (1999). New approaches to understanding p53 gene tumor mutation spectra. Mutat. Res. *43*, 199–209.

Johnstone, R.W., Ruefli, A.A., and Lowe, S.W. (2002). Apoptosis: a link between cancer genetics and chemotherapy. Cell *108*, 153–164.

Jurgensmeier, J.M., Xie, Z., Deveraux, Q., Ellerby, L., Bredesen, D., and Reed, J.C. (1998). Bax directly induces release of cytochrome c from isolated mitochondria. Proc. Natl. Acad. Sci. USA *95*, 4997–5002.

Kokontis, J.M., Wagner, A.J., O'Leary, M., Liao, S., and Hay, N. (2001). A transcriptional activation function of p53 is dispensable for and inhibitory of its apoptotic function. Oncogene *20*, 659–668.

Lowe, S.W., Schmitt, E.M., Smith, S.W., Osborne, B.A., and Jacks, T. (1993). p53 is required for radiation-induced apoptosis in mouse thymocytes. Nature *362*, 847–849.

Marchenko, N.D., Zaika, A., and Moll, U.M. (2000). Death signal-induced localization of p53 protein to mitochondria. A potential role in apoptotic signaling. J. Biol. Chem. *275*, 16202–16212.

Matsuda, K., Yoshida, K., Taya, Y., Nakamura, K., Nakamura, Y., and Arakawa, H. (2002). p53AIP1 regulates the mitochondrial apoptotic pathway. Cancer Res. *62*, 2883–2889.

Nakano, K., and Vousden, K.H. (2001). PUMA, a novel proapoptotic gene, is induced by p53. Mol. Cell *7*, 683–694.

Oda, E., Ohki, R., Murasawa, H., Nemoto, J., Shibue, T., Yamashita, T., Tokino, T., Taniguchi, T., and Tanaka, N. (2000). Noxa, a BH3-only member of the Bcl-2 family and candidate mediator of p53-induced apoptosis. Science *288*, 1053–1058.

Sansome, C., Zaika, A., Marchenko, N.D., and Moll, U.M. (2001). Hypoxia death stimulus induces translocation of p53 protein to mitochondria. Detection by immunofluorescence on whole cells. FEBS Lett. *488*, 110–115.

Schuler, M., and Green, D.R. (2001). Mechanisms of p53-dependent apoptosis. Biochem. Soc. Trans. *29*, 684–688.

Vakser, I.A., and Nikiforovich, G.V. (1995). Global range molecular matching program protein docking in the absence of detailed molecular structures. In Methods in Protein Structure Analysis, M.Z. Atassi and E. Appella, eds. (New York: Plenum Press), pp. 505–514.

Wagner, A.J., Kokontis, J.M., and Hay, N. (1994). Myc-mediated apoptosis requires wild-type p53 in a manner independent of cell cycle arrest and the ability of p53 to induce p21waf1/cip1. Genes Dev. *8*, 2817–2830.

Wang, X. (2001). The expanding role of mitochondria in apoptosis. Genes Dev. *15*, 2922–2933.

Wei, M.C., Lindsten, T., Mootha, V.K., Weiler, S., Gross, A., Ashiya, M., Thompson, C.B., and Korsmeyer, S.J. (2000). tBID, a membrane-targeted death ligand, oligomerizes BAK to release cytochrome c. Genes Dev. *14*, 2060–2071.

Wolter, K.G., Hsu, Y.T., Smith, C.L., Nechushtan, A., Xi, X.G., and Youle, R.J. (1997). Movement of Bax from the cytosol to mitochondria during apoptosis. J. Cell Biol. *139*, 1281–1292.

Xue, L., Chu, F., Cheng, Y., Sun, X., Borthakur, A., Ramarao, M., Pandey, P., Wu, M., Schlossman, S.F., and Prasad, K.V. (2002). Siva-1 binds to and inhibits BCL-X(L)-mediated protection against UV radiation-induced apoptosis. Proc. Natl. Acad. Sci. USA *99*, 6925–6930.

Yan, Y., Shay, J.W., Wright, W.E., and Mumby, M.C. (1997). Inhibition of protein phosphatase activity induces p53-dependent apoptosis in the absence of p53 transactivation. J. Biol. Chem. *272*, 15220–15226.

Yu, J., Zhang, L., Hwang, P.M., Kinzler, K.W., and Vogelstein, B. (2001). PUMA induces the rapid apoptosis of colorectal cancer cells. Mol. Cell *7*, 673–682.

Zhao, R., Gish, K., Murphy, M., Yin, Y., Notterman, D., Hoffman, W.H., Tom, E., Mack, D.H., and Levine, A.J. (2000). Analysis of p53-regulated gene expression patterns using oligonucleotide arrays. Genes Dev. *14*, 981–993.

Zong, W.X., Lindsten, T., Ross, A.J., MacGregor, G.R., and Thompson, C.B. (2001). BH3-only proteins that bind pro-survival Bcl-2 family members fail to induce apoptosis in the absence of Bax and Bak. Genes Dev. *15*,1481–1486.